Journal of the Geological Society, London, Vol. **171**, 2014, pp. 673–687. http://dx.doi.org/10.1144/jgs2013-107
Published *Online First* on July 23, 2014; updated July 31, 2014

Widespread Cretaceous secondary magnetization in the High Atlas (Morocco). A common origin for the Cretaceous remagnetizations in the western Tethys?

S. TORRES-LÓPEZ[1*], J. J. VILLALAÍN[1], A. M. CASAS[2], H. EL OUARDI[3], B. MOUSSAID[3] & V. C. RUIZ-MARTÍNEZ[4]

[1]*Departamento de Física, Escuela Politécnica Superior, Universidad de Burgos, Avd Cantabria S/N, 09006 Burgos, Spain*
[2]*Departamento de Ciencias de la Tierra, Facultad de Ciencias, Universidad de Zaragoza, 50009 Zaragoza, Spain*
[3]*Département de Géologie, Faculté des Sciences, Université Moulay Ismail, BP 11201 Zitoune, Meknès, Morocco*
[4]*Departamento de Geofísica y Meteorología, Facultad de Física, Universidad Complutense de Madrid, Avda. Complutense s/n, 28040 Madrid, Spain*
**Corresponding author (e-mail: storres@ubu.es)*

Abstract: In this paper, we present the first palaeomagnetic data (51 sites) for Mesozoic (Lower–Middle Jurassic) sediments of the Moroccan Central High Atlas and address the study of a widespread remagnetization. The remagnetization is characterized by a very stable component with systematic normal polarity, carried by magnetite. The relationship between the magnetic properties and location within the basin suggests that the acquisition of the remagnetization is controlled by basin geometry. Fold-tests indicate that the overprint acquisition is syn-folding in some structures but clearly predates the Tertiary compressional stage. Using the small circle intersection method we have calculated the remagnetization direction (D = 336.4°, I = 29.2°). Comparison with the global apparent polar wander path indicates that the remagnetization was acquired during the Late Cretaceous (probably Cenomanian). Considering both the basinal confinement of remagnetization and the connection with other remagnetization events in the western Tethys, we propose a scenario explaining widespread remagnetizations in the region, concerning both basin-scale conditions mainly related to sediment thickness and a regional-scale thermal event acting as catalyst of remagnetizations in those sedimentary basins that satisfy the basin-scale conditions.

Secondary magnetizations or remagnetizations are linked to various tectonic processes and basinal histories: volcanism or hydrothermal activity (Valet *et al.* 1998; Evans *et al.* 2000), burial and diagenesis (Katz *et al.* 1998; Woods *et al.* 2000; Gong *et al.* 2008*b*), low-grade metamorphism (Appel *et al.* 2012), thermal processes at the plate scale (Juárez *et al*. 1998) or wholesale thrusting during orogenic evolution (Stamatakos *et al.* 1996; Enkin *et al.* 1997, 2000; Lewchuk *et al.* 2002; Oliva-Urcia *et al*. 2007). The first references to 'remagnetization' can be found in the 1960s but it is especially from the 1980s that numerous studies about remagnetizations were published (Scotese *et al.* 1982; Kent 1985; Tucker & Kent 1988; McCabe & Elmore 1989). Most of them were performed in sedimentary rocks (limestones, marls or red beds), as identification of remagnetizations is easier when fold- or conglomerate-tests can be performed. Furthermore, in many cases, remagnetizations are linked to fluid circulation, and the higher permeability of sedimentary rocks allows for solution–precipitation of new magnetic phases. An overview of the remagnetization phenomenon has been given by Van der Voo & Torsvik (2012).

The study of remagnetizations presents particular problems in relation to the study of primary magnetizations. Probably the most important is related to determining the age of secondary magnetization, as some of the classical tests used for characterization of primary magnetizations do not allow this age to be constrained. Indirect procedures are the relationship with folding, the homogeneous polarity or the relationship with other basinal or thermal processes (Cairanne *et al.* 2002; Villalaín *et al.* 2003; Donald *et al.* 2006; Tohver *et al.* 2008).

In this paper we present a palaeomagnetic study on sedimentary rocks from the Moroccan High Atlas. The advantages of exploring this area from the palaeomagnetic point of view lie in (1) the thickness of Mesozoic deposits (specifically Jurassic), which reaches several thousand metres and thus favours the possibility of existence of remagnetizations and of sampling different portions of the sedimentary sequence, (2) its relatively well-known geological structure, (3) the geological evolution of the area, with a stage of tectonic inversion, which allows us to test the age of magnetizations and favoured the exhumation and outcrop of extensive sequences of the synrift units, and (4) the well-defined and widespread Mesozoic arm of the apparent polar wander path (APWP) for Africa, which allows indirect dating of palaeomagnetic vectors. In this study, we provide new palaeomagnetic results (51 new sites and about 500 samples) from the High Atlas, where no previous palaeomagnetic studies on Mesozoic sediments have been conducted. The Mesozoic basins of the High Atlas are susceptible to remagnetization because of their above-described characteristics. From the palaeomagnetic data, we interpret the magnetic properties and their relationship to the structure of the basin. Our results can provide information about the origin of the remagnetization and shed light on the problem of remagnetizations in the region of the western Tethys.

Geological framework

The Atlas is an intracontinental mountain chain developed over a continental basement (Mattauer *et al.* 1977; Frizon de Lamotte *et al.* 2000), which extends for 2000 km with ENE–WSW and east–west directions, from the Atlantic coast of Morocco to the Mediterranean, and defines the southernmost part of the Mediterranean Alpine system. There are two chains: the Middle Atlas, with NE–SW direction, and the High Atlas, with east–west direction. The Atlas chains developed as a result of the inversion of

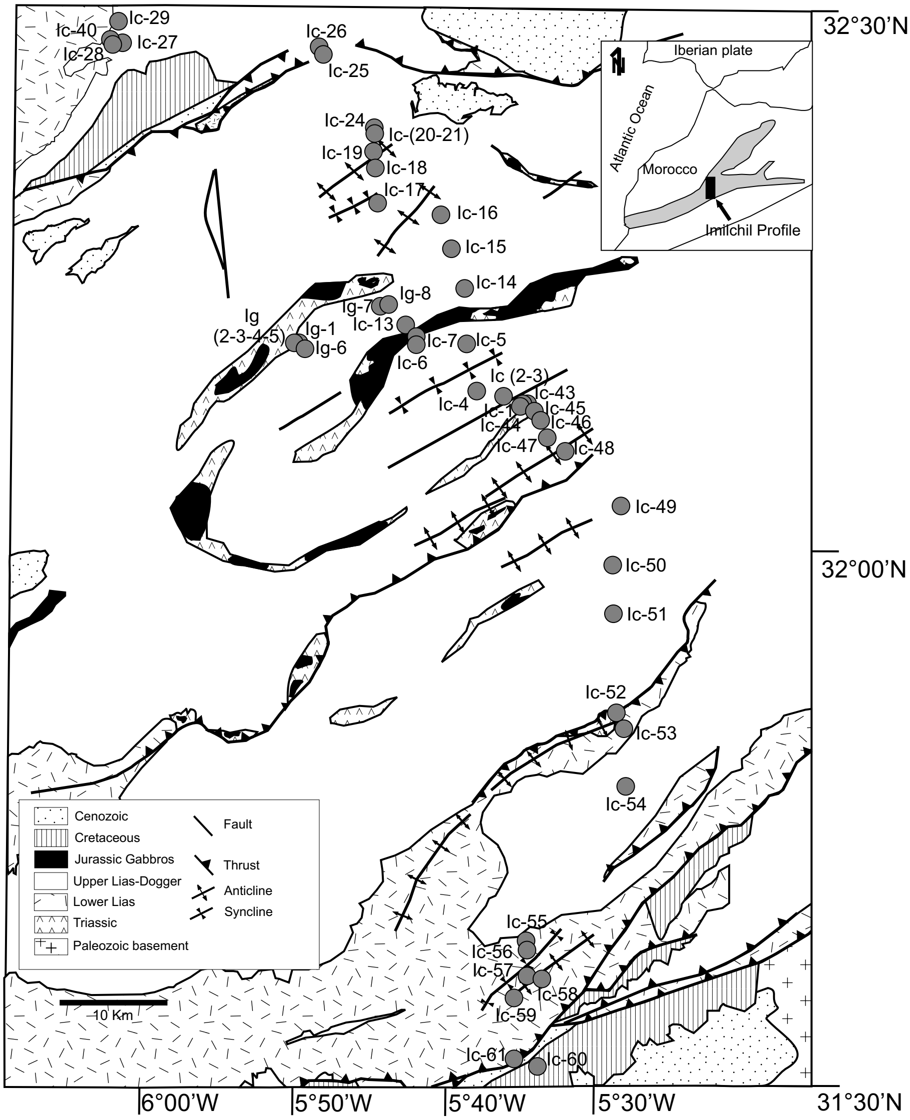

Fig. 1. Geological sketch map of the High Atlas showing the location of the Imilchil profile and the sampling sites.

the extensional or transtensional Mesozoic basins, as a consequence of the convergence between Africa and Europe during the Cenozoic (Mattauer *et al.* 1977). The amount of tectonic shortening and the uplift associated with the Alpine compression is still under discussion. Despite showing elevations of more than 4000 m, the Atlas has experienced moderate shortening. Some researchers have considered that thermal uplift, related to thinned lithosphere and mantle processes, has made a significant contribution to the relief of the High Atlas (Teixell *et al.* 2003; Ayarza *et al.* 2005; Zeyen *et al*. 2005).

Two rifting stages took place during the Triassic and Late Liassic–Dogger. The first stage, during the Triassic, is characterized by successive extensional episodes in a rifting context, controlling the subsequent evolution of the basins; these numerous episodes are represented by red beds units with intercalated basaltic lava flows (Choubert & Faure-Muret 1962; Piqué *et al.* 2000), which were deposited in graben structures and ended abruptly against their margins. In the second extensional stage, during the Jurassic, basins were elongated in NE–SW (Mattauer *et al.* 1977) and ENE–WSW (Laville & Piqué 1992) directions. The second rifting evolution is evidenced by lithostratigraphic changes, which show bathymetric or environmental variations from deep to shallow water, and lasted from the Middle Liassic until the Dogger (Frizon de Lamotte *et al.* 2008). During the Early Jurassic, shallow marine platforms, with increasing subsidence, controlled the deposition of carbonates. The Middle Jurassic was characterized by deposition of marl–limestone series, ending with a marine regression and the sedimentation of red bed deposits. The Middle Jurassic represents the episode with maximum subsidence and thickness of sediments, reaching more than 5000 m (Laville *et al.* 1977; Ibouh *et al.* 1994; Teixell *et al.* 2003) in the basin centre. A phase of compressive folding and erosion, witnessed by unconformities and pervasive structures at the outcrop scale, was proposed for the Late Jurassic by Mattauer *et al*. (1972, 1977), Laville & Piqué (1992) and Laville *et al*. (2004). However, this compressional, intermediate stage is still controversial and not recognized by other researchers (see, e.g. Frizon de Lamotte *et al.* 2008). In the Middle and Late Jurassic, an alkaline-type magmatic episode, forming intrusions of igneous rocks along a N45°E axis (Laville & Piqué 1992), took place in the central part of the High Atlas (Fig. 1). This magmatic episode is characterized by gabbro intrusions and basaltic lava flows, prior to the Aptian extensional episode (Laville & Harmand 1982; Laville & Piqué 1992; Barbero *et al.* 2007; Frizon de Lamotte *et al.* 2008). The Late Cretaceous presents local evidence of folding that, for some researchers, indicates the first Alpine compression stages in the Atlas (Laville *et al.* 1977; Mattauer *et al.* 1977; Laville 2002). Generalized basin inversion took place during two compressive episodes: the first occurred in the Late Eocene and the second from the Late Miocene to the present (El Harfi *et al.* 2001, 2006; Bracène & Frizon de Lamotte 2002; Missenard 2006; Frizon de Lamotte *et al.* 2008).

The Cenozoic deposits are alluvial and lacustrine conglomerates that are contemporaneous with the main compressional deformation. Cenozoic magmatism with alkaline and hyper-alkaline affinity, related to mantle uplift, formed volcanic and sub-volcanic rocks (Teixell *et al*. 2005).

The tectonic style characterizing the High Atlas is mainly thick-skinned, as the basement was involved in the compressional deformation (Frizon de Lamotte *et al.* 2000; Teixell *et al.* 2003; El Harfi *et al.* 2006). However, there are structures in its southern border that have been interpreted as having evolved within a thin-skinned style of deformation (Beauchamp *et al.* 1999; Benammi *et al.* 2001; Teixell *et al.* 2003), favoured by the existence of low-strength detachment levels within the Mesozoic series. Compressional deformation is heterogeneously distributed: narrow anticlines or thrust faults with clearly Tertiary compressional origin are separated by broad synclines that can be interpreted as the result of extensional tectonics, Mesozoic compressional events or Tertiary, Atlasic movements. Variations in Mesozoic stratigraphy and thickness of the Mesozoic series across many thrust faults attest to their origin as synsedimentary extensional faults (Frizon de Lamotte *et al.* 2000). Thrust-related folds are also characteristic of the deformation pattern affecting Jurassic rocks and the Upper Cretaceous–Eocene series; in the Central High Atlas, thrusts are oriented NE–SW to N70E, parallel to the South Atlas Fault zone (Ellero *et al.* 2012). Kinematic analysis suggests that thrusting and folding can be also linked to the development of strike-slip faulting in a complex polyphase tectonic evolution.

Palaeomagnetic methods and sampling

A total of 51 sites, with 8–11 samples per site, were sampled along the Imilchil cross-section (*c*. 90 km), one of the classical transects in the High Atlas, with a NNW–SSE direction (Fig. 1). The sampled series consists of Jurassic limestones and marly limestones, with ages between Sinemurian and Bathonian, except for two sites located in Cretaceous sandstones of Valanginian age (Fig. 2). Sampled sites (Fig. 2a) are distributed along large-scale structures (Fig. 2b), gabbro outcrops and diapirs related to Triassic materials (Fig. 2c) and small-scale folds (Fig. 2d and e). The sampling sites include depocentral areas, and the two margins (NW and SE) of the Jurassic basin, where the thickness of the Mesozoic sequence decreases dramatically.

Sampling was carried out by means of a gasoline portable drilling machine and samples were oriented using a magnetic compass–inclinometer device. All the palaeomagnetic and rock magnetic analyses were carried out in the Palaeomagnetism Laboratory of the University of Burgos (Spain). The natural remanent magnetization (NRM) of about 500 samples was measured using a 2G755 cryogenic magnetometer. Stepwise thermal demagnetization was carried out with a TD48-SC thermal demagnetizer. This technique was systematically used in samples from all cores. In addition, pilot samples, one or two for each station, were demagnetized using the alternating field (AF) technique. The steps for AF demagnetization followed progressive peak fields, applying increasing fields of 2–10, 5–30, 10–60 and 20–100 mT. Thermal demagnetization was carried out in steps of 25 °C up to 575 °C except for some samples that reached 700 °C. Low field magnetic susceptibility was monitored during the demagnetization process with a KLY4S susceptibility bridge (AGICO Kappabridge), to detect mineralogical changes induced by thermal treatment.

After the magnetic analyses, magnetic components were isolated using linear regression techniques. The distribution of directions was determined using the statistics of Fisher (1953). To analyse the stability of the magnetic components, several fold-tests in large-scale and metre-scale folds were performed. The statistical confidence of the fold-tests was determined by the McFadden & Jones (1981) method. To determine the properties of the carriers of the magnetization, several rock magnetic experiments were performed. Representative samples were submitted to progressive acquisition of isothermal remanent magnetization (IRM) using a pulse magnetizer, reaching a maximum field of 2 T. Furthermore, samples were thermally demagnetized after they had acquired three orthogonal IRM components under fields of 2, 0.4 and 0.12 T (Lowrie 1990). Thermomagnetic and backfield curves, as well as hysteresis loops, have been determined by means of a magnetic variable field translation balance (MMVFTB).

Palaeomagnetic analysis

On the basis of palaeomagnetic properties, two types of behaviour (G1 and G2) can be distinguished. Group G1 corresponds mainly to marine and lacustrine Jurassic limestones, and shows uniform magnetic characteristics, independently of stratigraphic position and lithology of samples. This group presents magnetic susceptibility values between 10 and 700×10^{-6} (S.I.), most of them between 100 and 400×10^{-6} (S.I.). The intensity of the NRM is very high, varying between 1 and 80 mA m^{-1}, with most samples having values between 20 and 40 mA m^{-1}.

Thermal demagnetization of the NRM of group G1 (Fig. 3a–f) revealed two stable components. One of them has a maximum unblocking temperature between 200 and 250 °C, and is aligned with the present-day Earth's magnetic field before any tectonic correction. We have considered it as a viscous (V) component. After removing the V component, a second component (A) with maximum unblocking temperatures of 450–475 °C (exceptionally 500 °C; Fig. 3a–d) and intermediate coercivities, between 30 and 100 mT (Fig. 3e and f), was identified. The A component is well defined and is very stable, presenting a systematic normal polarity. In this study we have considered the A component as the characteristic remanent magnetization (ChRM).

The component A (group G1) is observed at most of studied sites (40 sites), distributed along the central area of the basin (70 km wide belt), south of the Tizi-n-Isly fault and north of the Zabel thrust faults, where the thickness of the Mesozoic series is greater (>5 km; Fig. 2a).

The second group of sites (G2) corresponds to similar stratigraphic ages and lithology, but with heterogeneous magnetic behaviour. Many of these samples showed very low intensities (0.01–1 mA m^{-1}) and susceptibility values between diamagnetic behaviour and $1–6 \times 10^{-6}$ (S.I.). These samples show very unstable demagnetization diagrams and erratic directions (Fig. 3i and j). Group G2 also includes two sites located at the northern basin border (Fig. 2a), showing high NRM intensities (5–20 mA m^{-1}) and two magnetic phases with maximum unblocking temperatures of 350 °C and 575 °C, respectively (Fig. 3g and h). Both phases show reversed polarities. Group G2 also includes two sites sampled in Cretaceous rocks, with high unblocking temperatures (680 °C) and scattered directions (Fig. 3k). The sites corresponding to G2 behaviour are located in the marginal areas of the basin, to the north of the Tizi-n-Isly fault and in the southern basin border (Zabel thrust fault complex).

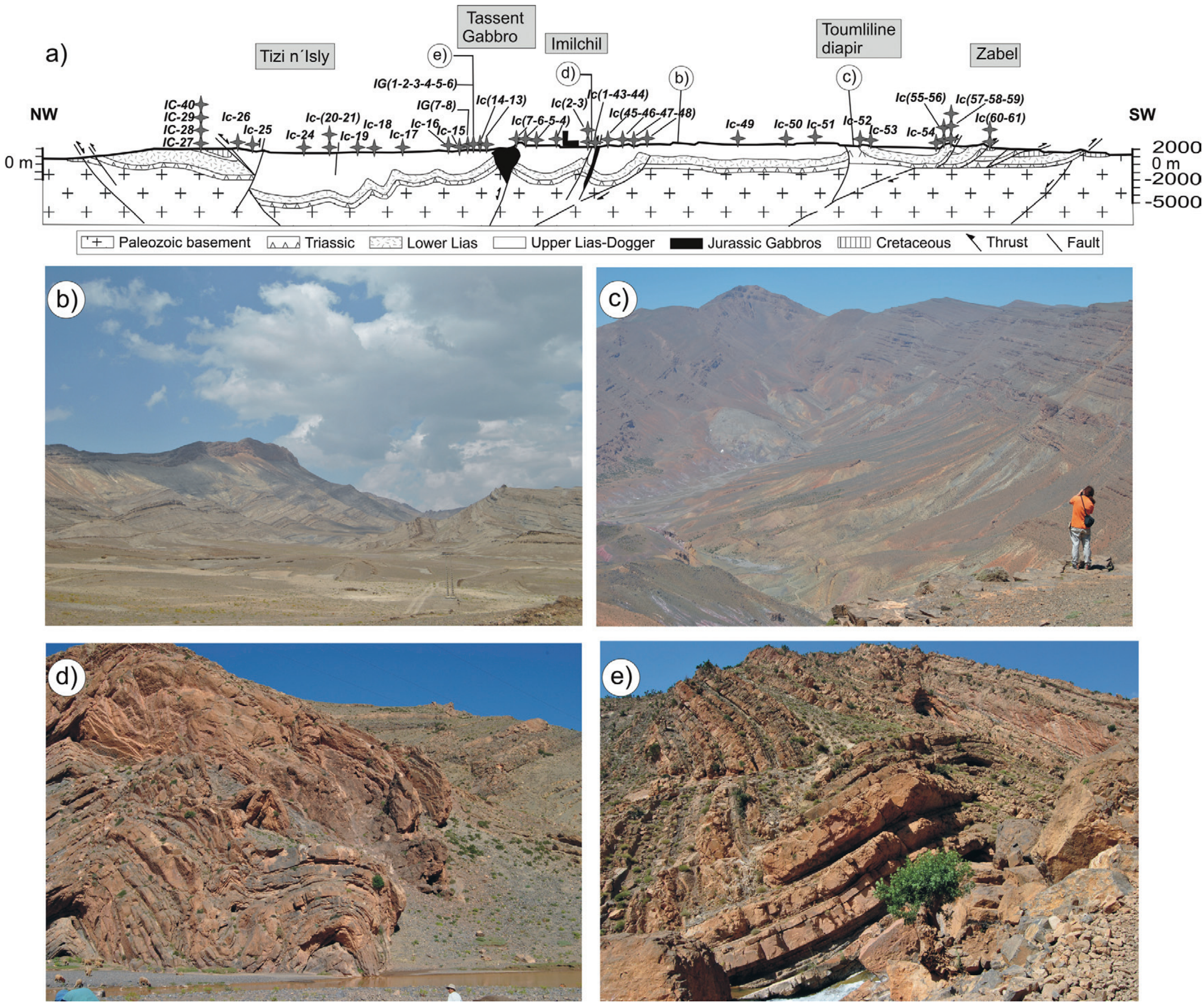

Fig. 2. (**a**) Geological cross-section (from Teixell *et al.* 2003) through the High Atlas of Morocco (Imilchil section) with the projection of the palaeomagnetic sites. Location of cross-section is shown in Figure 1. (**b**, **c**) Examples of synrift structures: kilometre-scale anticline (ridge) located south of Imilchil (**b**) and Toumliline diapir (**c**). (**d**, **e**) Examples of Tertiary compressional folds, located close to IC2–IC3 sites (**d**) and at the IG(2, 3, 5) site with fold-test (**e**).

Magnetic mineralogy

The acquisition of IRM for group G1 (Fig. 4a, b, d and e) indicates that magnetization is saturated below fields of 0.5 T, suggesting that the dominant magnetic carriers have low coercitivity. At a few sites, another small, high-coercitivity contribution is observed (Fig. 4e). In the thermal demagnetization of three IRM components, the low-coercivity phase shows drops at unblocking temperatures between 475 and 525 °C, suggesting that magnetite is the main carrier. The rare high-coercitivity phases show unblocking temperatures of 675 °C, characteristic of hematite (Fig. 4e).

The thermomagnetic curves of samples from group G1 (Fig. 4c and f) show very clear drops at 580 °C, which confirm the presence of magnetite observed in the IRM experiments (Fig. 4f). In some samples, an increment at 450 °C could be connected to development of secondary magnetite (Fig. 4c), probably owing to oxidation of pyrite, which is very abundant in these rocks. A small drop at 300 °C (i.e. Fig. 4f) that could be caused by several reasons (e.g. the presence of ferromagnetic sulphides such as greigite and pyrrhotite) has also been detected. The magnetic mineralogy of group G2 is very heterogeneous. Some sites become saturated at fields below 1 T and the intermediate-coercivity curve of the thermal demagnetization presents maximum unblocking temperatures of 325–350 °C, which indicate the presence of ferromagnetic sulphides, greigite or pyrrhotite. The low-coercivity phase shows the presence of magnetite with maximum unblocking temperature of 575 °C (Fig. 4g).

The presence of sulphides is also confirmed by the thermomagnetic curve (Fig. 4i), which shows a sharp drop at 350 °C, probably owing to the presence of pyrrhotite, because this drop is also observed in the cooling curve. A significant drop can also be observed at 580 °C, indicating the Curie temperature of magnetite. There are sites that do not saturate when reaching 2 T fields, indicating the presence of hematite, although during the IRM thermal

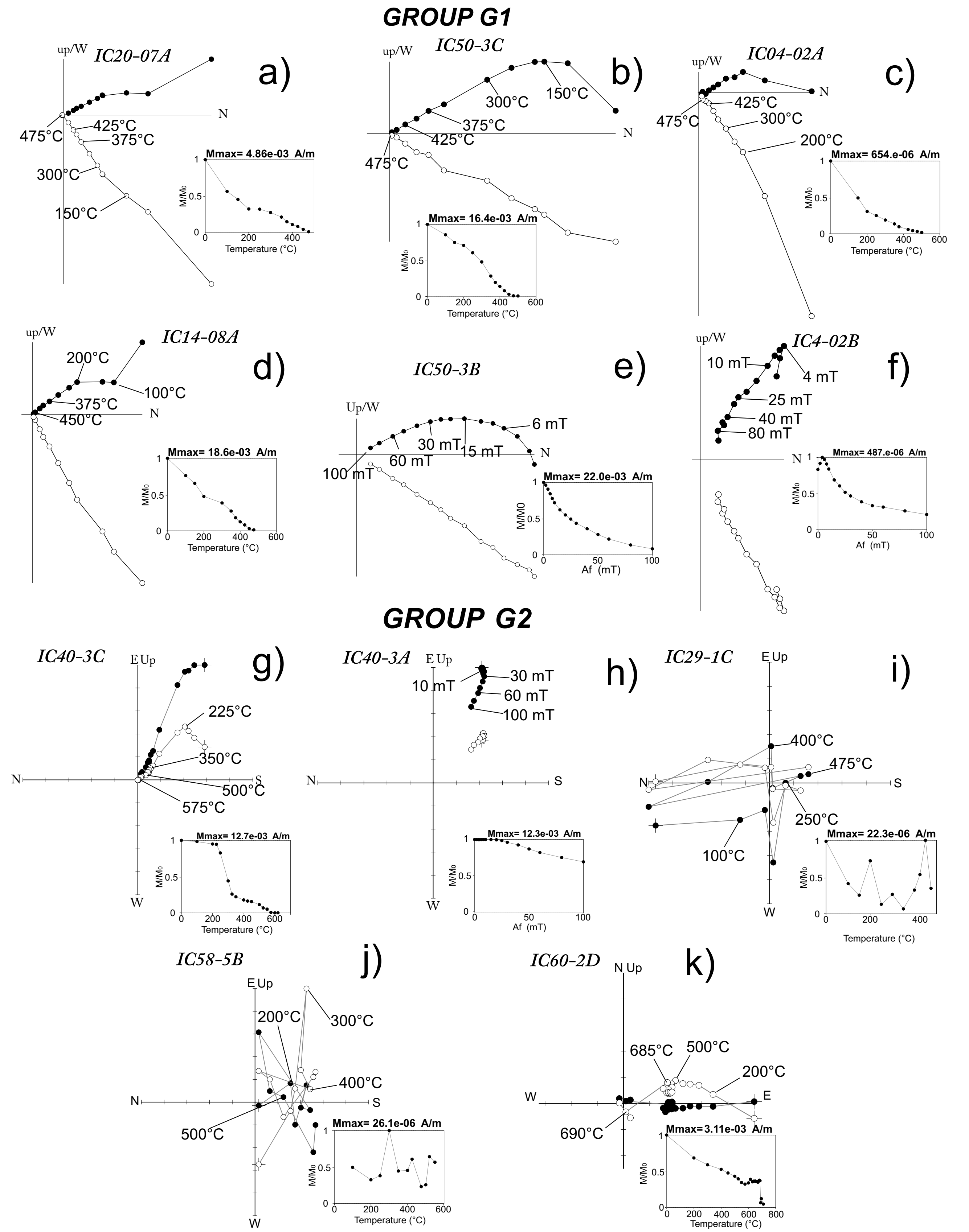

Fig. 3. NRM thermal and alternating field demagnetizations of representative samples of groups G1 and G2. All directions are plotted in *in situ* coordinates. Open symbols are projections of the vector end points onto the vertical north–south or east–west plane and filled symbols are projections onto the horizontal plane. The evolution of normalized NRM intensity M/M_0 is also shown in the insets.

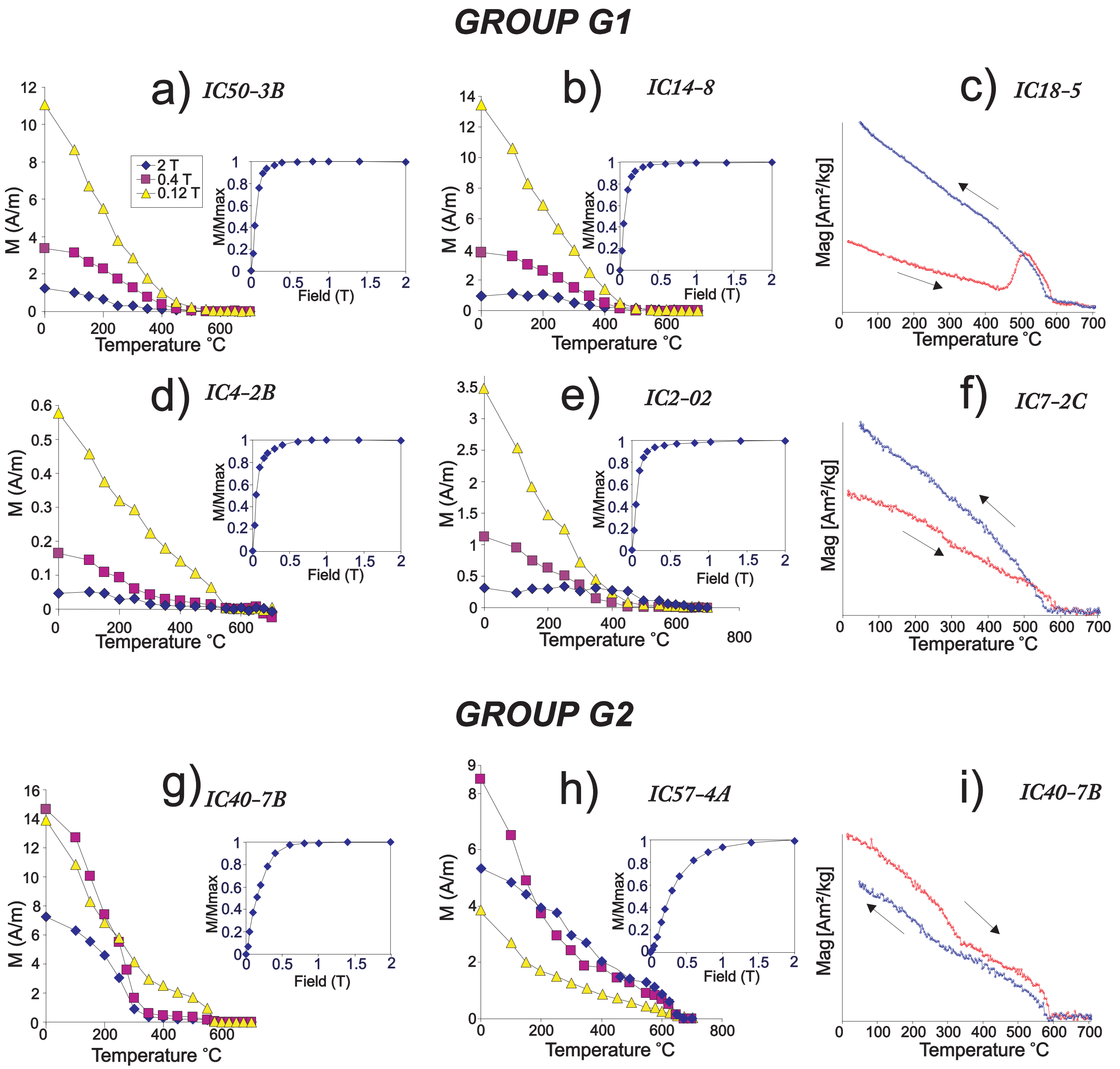

Fig. 4. IRM acquisition and subsequent thermal demagnetization of three orthogonal IRM components of representative samples of groups G1 and G2 (**a**, **b**, **d**, **e**, **g**, **h**). Thermomagnetic curves of induced magnetization of representative samples of both groups are also shown (**c**, **f**, **i**).

demagnetization the low-coercivity component shows a drop at temperatures of 550 °C, indicating also the presence of magnetite (Fig. 4h).

Samples show 'wasp-waisted' hysteresis loops (Fig. 5), which are considered indicative of a bimodal distribution of grains with contrasting coercivity, probably related to differences in grain size (Jackson 1990; Roberts *et al.* 1995). The parameters of hysteresis M_r/M_{rs} and H_{cr}/H_c (Fig. 5) of G1 samples are within the SD + SP mixture area (Dunlop 2002) with approximate limits of $0.1 < M_{rs}/M_s < 0.5$ and $3 < H_{cr}/H_c < 20$. All in all, they show a very similar behaviour to remagnetized limestones that have been interpreted as carrying a chemical remagnetization (Jackson 1990; Channell & McCabe 1994).

Analysis of palaeomagnetic directions

Only component A, observed in the sites of group G1, can be analysed from the directional point of view to obtain reliable palaeomagnetic vectors. It was identified at 40 out of 51 stations (Fig. 6 and Table 1).[Setter: no link is possible to Table 1. Please add the link] The directions obtained show strong scatter both before and after bedding correction. The palaeomagnetic vectors are distributed in a vertical plane with a NW–SE direction, with a strong scatter in inclination. All sites systematically present normal polarity. Taking into account that normal and reverse polarities are expected for the Jurassic period, the single polarity nature of this component and the dispersion observed before and after bedding correction

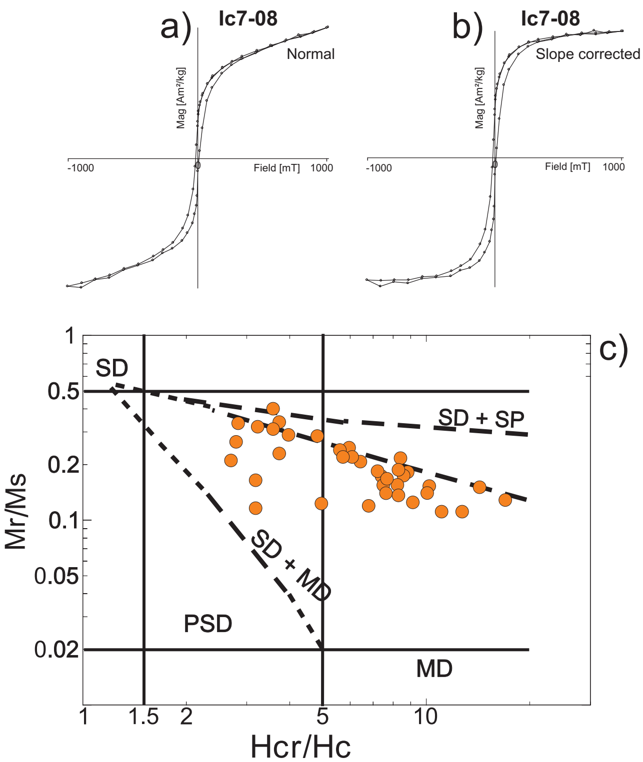

Fig. 5. (**a**, **b**) Hysteresis loops before and after slope correction of a representative sample of group G1. (**c**) Day diagram (Day *et al.* 1977), showing the hysteresis parameters for representative samples from group G1. SD, single domain; PSD, pseudo-single domain; MD, multidomain; SP, superparamagnetic. Dashed lines indicate the theoretical reference lines following Dunlop (2002) for SD + SP and SD + MD.

suggest that the characteristic component A is not a primary magnetization, but a remagnetization. The scatter of palaeomagnetic vectors before and after tectonic correction suggests a syn-folding remagnetization. However, it must be understood that a syn-folding remagnetization does not strictly imply that it was acquired during the development of a single, compressional fold (see, e.g. Villalaín *et al.* 1994), In the High Atlas, a tectonic quiescent period between the end of synrift sedimentation (Early Cretaceous) and the onset of collision-related compression during the Tertiary is generally acknowledged (see Michard *et al*. 2008, and references therein). Therefore, the events occurring between synrift deformation (here including folding associated with normal faults, diapirs and igneous intrusions; Teixell *et al.* 2003; Michard *et al.* 2008, Fig. 2b and c) and wholesale compressional folding and thrusting (Fig. 2d and e) during the Tertiary can be considered as 'syn-folding' *sensu lato*, because the present-day tilting of beds (i.e. finite deformation) reflects the whole sequence of events occurring after sedimentation and early diagenesis.

To assess the stability of the A component and to determine the relative age of the remagnetization in relation to some structures, several fold-tests were performed along the cross-section in metre-scale and kilometre-scale folds. Because in the inner part of the fold belt there are no syncompressional sediments that would allow us to unequivocally date the age of folding, indirect indicators such as the geometry of folds and their relationships with extensional faults must be used to assign a tentative age to folds. Furthermore, the study of remagnetizations provides a feedback for quantifying the amount of tilting in the pre- and post-remagnetization stage (see Villalaín *et al.* 2003). Indeed, the fold-test results indicate pre-folding and syn-folding acquisition of the remagnetization depending on the type and geometry of the analysed structure, as described below.

The fold-test performed in tight, metre-scale folds, probably related to the Tertiary compression (Fig. 2d and e) indicates a clear pre-folding acquisition (Fig. 7a). Sites lg2 and lg3 correspond to the limbs, and site lg5 corresponds to the hinge zone. In this case, the directions are scattered before and clustered after tectonic correction, giving a pre-folding acquisition at 95% level of confidence (McFadden & Jones 1981). The fold-test carried out in a kilometre-scale syncline (sites Ic4, Ic5, Ic6; Fig. 2b) suggests acquisition of remagnetization at an intermediate deformation stage, as directions are scattered before and after tectonic correction (Fig. 7b). In the incremental fold-test we observe that the maximum grouping takes place at an unfolding configuration of 50%, corresponding to a minimum *f* value (McFadden & Jones 1981), indicating that both distributions present statistically the same direction at 95% level of confidence in the curve (Fig. 7b). Because large-scale synclines in this transect are confined between anticlinal ridges that can be linked in some cases to extensional faults or other synrift structures, the tilting in the southern limb of this syncline (site Ic4) is

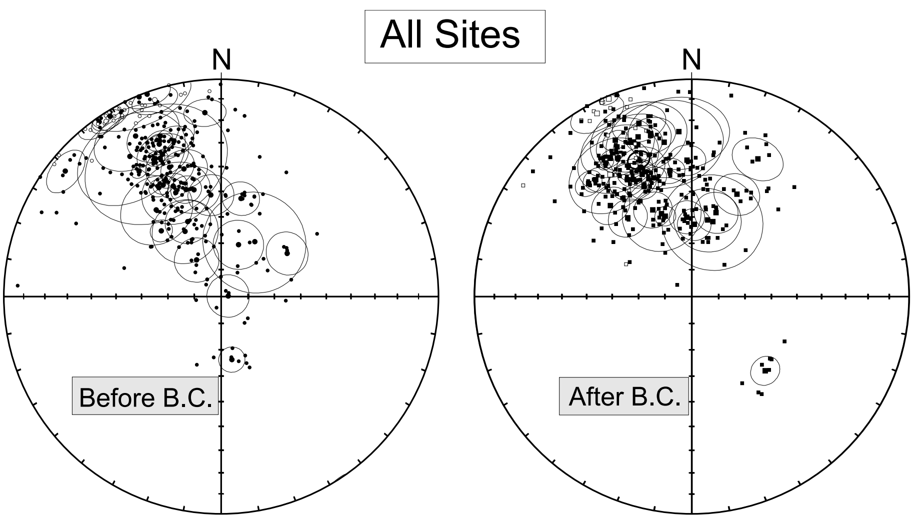

Fig. 6. Equal-area projections showing directions for characteristic magnetization (component A) obtained in all samples before and after bedding correction (B.C.). Mean direction and 95% confidence circle are also represented for each site. Filled symbols are plotted on lower hemisphere and open symbols on upper hemisphere.

Table 1. *Remanent magnetization parameters for the characteristic component*

Site	Age	Latitude (°N)	Longitude (°W)	*In situ* bedding (*DD/D*)	N/N_0	*In situ*				100% tilt corrected			
						D	*I*	*k*	α_{95}	*D*	*I*	*k*	α_{95}
IC-2	Bajocian	32.156	5.598	178, 42	7/8	325.6	–2.7	170.4	4.6	320.7	31.2	170.3	4.6
IC-3	Bajocian	32.156	5.598	338, 66	7/8	85.0	87.4	59.0	7.9	345.8	24.5	59.2	7.9
IC-4	Bathonian	32.162	5.630	348, 22	8/8	336.4	46.6	21.6	12.2	337.0	25.6	21.6	12.2
IC-5	Bajocian	32.208	5.640	168, 54	7/9	339.9	1.3	90.2	6.4	335.8	54.0	76.6	6.9
IC-6	Bajocian	32.207	5.695	155, 35	8/10	338.4	24.2	167.5	4.3	341.9	60.2	213.8	3.8
IC-7	Aalenian	32.214	5.697	149, 81	8/10	341.8	47.2	105.6	5.4	135.9	53.7	105.5	5.4
IC-13	Toarcian	32.225	5.704	343, 33	7/8	336.1	31.3	502.5	2.7	337.2	–1.5	512.8	2.7
IC-14	Aalenian	32.269	5.643	355, 40	8/10	317.5	56.6	181.8	4.1	333.9	21.0	181.8	4.1
IC-15	Aalenian	32.299	5.657	164, 09	8/8	342.5	29.8	166.4	4.3	342.3	38.8	166.4	4.3
IC-16	Aalenian	32.330	5.665	090, 00	7/8	336.5	44.0	75.9	7.0	336.5	44.0	75.9	7.0
IC-17	Aalenian	32.342	5.739	326, 15	8/9	330.1	42.0	244.0	3.6	329.4	27.1	244.0	3.6
IC-18	Toarcian	32.378	5.742	146, 36	8/8	343.1	26.3	76.0	6.4	356.4	60.0	76.4	6.4
IC-19	Aalenian	32.392	5.741	328, 82	8/8	170.3	65.8	133.0	4.8	317.6	30.2	132.9	4.8
IC-20	Bajocian	32.408	5.740	340, 35	7/8	325.9	73.7	53.9	8.3	333.3	39.5	52.9	8.4
IC-21	Bajocian	32.408	5.740	138, 54	7/8	341.3	–5.3	86.0	6.5	350.0	40.9	137.7	5.2
IC-24	Bathonian	32.414	5.743	018, 12	7/8	332.5	41.9	273.5	3.7	338.7	33.0	273.5	3.7
IC-25	Bajocian–Bathonian	32.484	5.796	155, 56	5/8	337.7	0.7	29.7	14.3	339.8	56.6	29.7	14.3
IC-26	Aalenian–Bajocian	32.495	5.804	351, 42	5/8	336.0	59.1	86.0	8.3	343.0	17.8	86.0	8.3
IC-43	Bathonian	32.134	5.577	092, 70	8/8	337.6	29.9	42.2	8.6	25.6	30.4	42.2	8.6
IC-44	Bathonian	32.150	5.579	115, 57	7/8	326.9	24.1	11.7	18.4	15.5	60.7	11.7	18.4
IC-45	Bathonian	32.141	5.569	090, 25	7/8	354.2	51.2	56.1	8.1	23.7	47.3	55.8	8.2
IC-46	Bathonian	32.135	5.560	324, 49	7/8	31.6	65.8	10.9	19.1	349.8	28.6	11.0	19.0
IC-47	Bathonian	32.118	5.550	342, 85	8/8	323.1	48.7	18.6	13.2	326.1	–32.9	15.2	14.7
IC-48	Toarcian	32.105	5.530	161, 51	7/8	328.4	2.9	119.9	5.5	320.8	51.4	71.6	7.2
IC-50	Aalenian	32.028	5.468	128, 10	9/10	334.6	30.4	273.1	3.1	337.9	39.2	273.1	3.1
IC-51	Bajocian	31.964	5.481	139, 18	9/10	337.9	25.3	136.6	4.4	342.2	42.1	136.5	4.4
IC-52	Sinemurian	31.870	5.476	313, 10	7/8	344.7	31.3	7.1	24.3	341.4	23.4	19.5	15.6
IC-53	Sinemurian	31.856	5.465	105, 39	9/10	308.8	8.8	53.9	7.1	318.1	43.2	54.9	7.0
IC-54	Aalenian–Bajocian	31.804	5.468	154, 11	7/8	331.9	17.5	20.3	13.7	331.8	28.4	20.3	13.7
IC-59	Sinemurian	31.602	5.586	336, 38	9/10	331.0	61.9	18.9	12.2	333.4	24.0	18.9	12.2
IG1	Aalenian	32.207	5.825	123, 40	10/10	325.1	2.3	56.1	6.5	331.4	28.7	54.6	6.6
IG2	Aalenian	32.208	5.828	130, 57	7/8	339.2	22.1	32.2	10.8	12.0	60.4	25.3	12.2
IG3	Aalenian	32.208	5.828	314, 24	6/8	56.9	60.2	72.3	7.9	16.5	56.9	72.3	7.9
IG4	Aalenian	32.208	5.828	320, 13	6/8	343.8	38.7	71.5	8.0	340.6	26.6	71.5	8.0
IG5	Aalenian	32.208	5.828	340, 10	5/8	18.4	69.5	68.7	9.3	2.3	62.8	155.8	6.1
IG6	Bajocian	32.205	5.822	129, 60	10/10	332.7	–5.9	28.1	9.3	345.7	47.9	37.7	8.0
IG7	Aalenian	32.244	5.733	160, 22	9/10	355.0	16.1	66.9	6.3	358.2	37.3	66.8	6.3
IG8	Aalenian	32.246	5.724	318, 16	9/10	9.6	52.4	61.6	6.6	356.4	41.4	11.3	16.0

DD/D, Dip direction and dip; N/N_0, number of sample directions used in the analysis versus number of samples demagnetized; *k* and α_{95}, Fisher statistical parameters (Fisher 1953); *D*, declination; *I*, inclination.

probably related to the movement of a normal fault during the extensional stage. This movement can be responsible for the pre-magnetization deformation detected in this syntectonic fold-test. In summary, the fold-test results indicate that component A is a remagnetization acquired before the compressional stages related to the inversion of the basin, but after some folding processes, such as the formation of synclines related to normal faulting.

Age of remagnetization

To determine the age of the remagnetization (component A) observed in rocks from the inner part of the basin (group G1) we must take into account several constraints: (1) the chronology relative to deformation inferred from fold-tests; (2) the systematic normal polarity; (3) the remagnetization direction; (4) the comparison with the global apparent polar wander path (GAPWP) (Torsvik *et al.* 2012) in NW Africa coordinates.

The fold-tests in the Imilchil transect indicate that the remagnetization was acquired before Alpine compression but after other tectonic events related to basin evolution, such as gabbro intrusions and synsedimentary folds associated with extensional tectonics.

A definitive chronological criterion can be obtained from the comparison of the palaeomagnetic direction with the GAPWP. For this purpose, a reliable direction must be obtained. Because the secondary magnetization is broadly syntectonic, directions obtained before or after tectonic correction cannot be directly used. The small circle intersection (SCI) method of Shipunov (1997) and Waldhör & Appel (2006) allows us to calculate the characteristic direction of a synfolding remagnetization. This method assumes that during tilting, the direction of magnetization rotates around a horizontal axis parallel to the bedding strike and then the magneti-

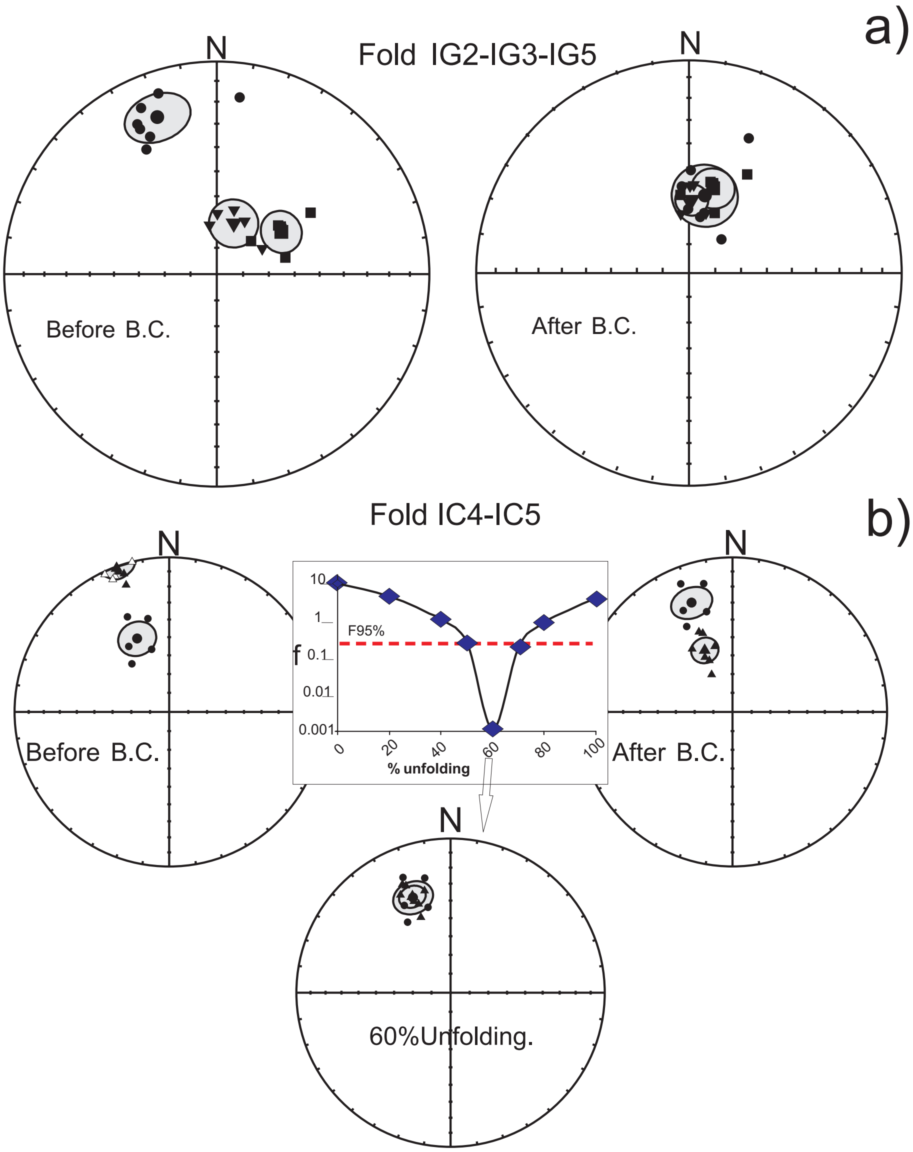

Fig. 7. (**a**) Fold-test in a metre-scale fold. Squares, small circles and triangles are directions corresponding to samples from different limbs before and after bedding correction (B.C.). Mean direction and 95% confidence circle are also shown. (**b**) Incremental fold-test in a kilometre-scale syncline. Small circles and triangles are directions corresponding to both limbs before and after bedding correction (BC) and to the 50% unfolding. Mean direction and 95% confidence circle are also shown. The parameter *f* (McFadden & Jones 1981) as a function of the percentage of unfolding of bedding tilt is represented in the graph. Horizontal dashed line represents the critical value of *f* at the 95% confidence level (F95%).

zation vector follows a small circle trajectory in its rotation around the bedding strike. The intersections of the small circles from different sites represent the single possible common magnetization direction (Shipunov 1997), which can be interpreted as the characteristic direction of remagnetization.

To increase the reliability of the direction obtained, a high number of intersections between small circles, and therefore a wide range of bedding strikes, must be present (see, e.g. Henry *et al.* 2004). Furthermore, the method assumes that no vertical-axis rotations occurred. The statistical solution is obtained by minimizing the sum $A = \Sigma|\alpha_M|$ of the angular distances (α_M) between the direction and each small circle (see Waldhör & Appel 2006). This method has been successfully used for finding the remagnetization characteristic direction in Mesozoic basins in Iberia (Soto *et al.* 2008, 2011; Casas *et al.* 2009; Gong *et al.* 2009).

Our data are appropriate for the use of this method because the intersection of the small circles shows a very narrow region in declination (Fig. 8a), there is no evidence of differential rotations around vertical axes between different parts of the transect and structures are generally coaxial (Teixell *et al.* 2003). From the 40 sites selected to calculate the remagnetization direction, we removed those with bedding dips lower than 10°, to avoid errors in the measurement of bedding strike. To avoid data with poor palaeomagnetic statistics, sites with $\alpha_{95} > 15°$ have been filtered. The result obtained for the direction of the remagnetization from 33 sites (Fig. 8b) is $D = 336.4°$ and $I = 29.2°$ ($k = 36.3$, $\alpha_{95} = 4.1°$).

To use the average direction obtained to constrain the age of remagnetization through comparison with the APWP of Africa in this area, vertical-axis rotations of the whole High Atlas should be discarded. According to palaeogeographical reconstructions (Sibuet *et al.* 2012) and the intracratonic features of the High Atlas, an overall rotation of the magnitude implied by the average palaeomagnetic vector, for the whole High Atlas, can be discarded. Furthermore, the recently published palaeomagnetic pole from the *c.* 200 Ma Central Atlantic Magmatic Province tholeitic basaltic lava sequence in the Argana basin agrees well with the poles derived for this province from NW Africa, implying that minor net movements since 200 Ma occurred in the Moroccan Meseta with respect to NW Africa (Ruiz-Martínez *et al.* 2012).

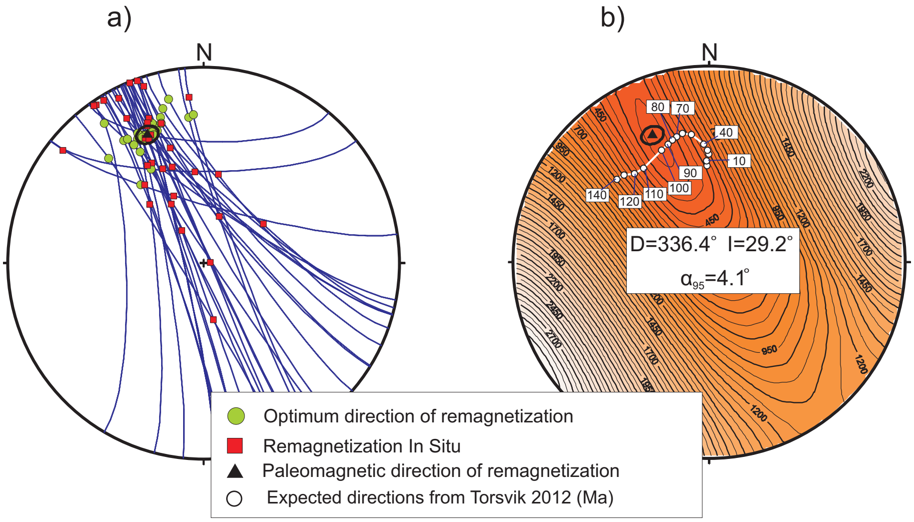

Fig. 8. (**a**) Small circles corresponding to remagnetization directions from selected sites. Circle symbols are the optimum directions of remagnetization for each site. Squares are directions of the *in situ* remagnetization for each site. Triangle shows the palaeomagnetic direction of remagnetization. The 95% confidence circle is also represented. (**b**) Equal area projection showing contours of equal value *A*. Triangle shows the maximum value of *A* ($A = \Sigma|\alpha_M|$). The 95% confidence circle is also represented. Further explanation has been given by Waldhör & Appel (2006). The curve in the *A* contours shows the expected palaeomagnetic directions at the Imilchil area from the GAPWP in Africa coordinates (Torsvik *et al.* 2012).

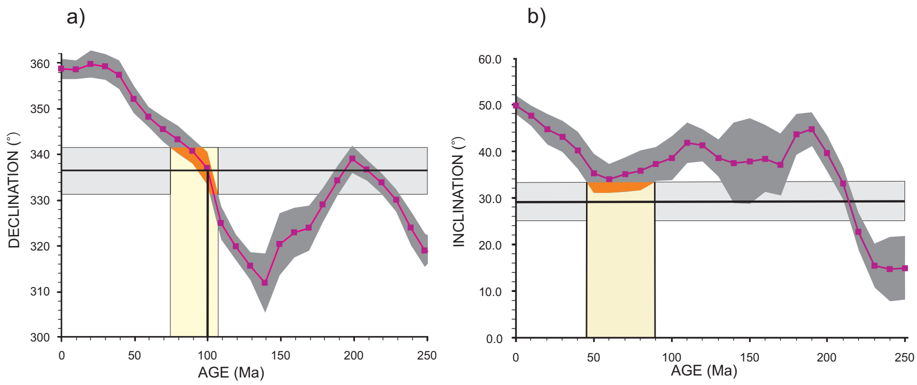

Fig. 9. Declination–age curve (**a**) and inclination–age curve (**b**) expected at the Imilchil area from the GAPWP in African coordinates (Torsvik *et al.* 2012). Uncertainties of the expected directions are shown. The horizontal lines represent the observed declination or inclination (and their uncertainties, calculated as $\Delta D = \alpha_{95}/\cos I$; $\Delta I = \alpha_{95}$) at the Imilchil cross-section. The vertical shaded region indicates the possible solutions.

The mean palaeomagnetic vector obtained for the Central High Atlas remagnetization can be compared with the expected directions for the Imilchil area obtained from the Mesozoic successive running means for the GAPWP, which have been rotated from South African to NW African coordinates for ages older than 130 Ma (Torsvik *et al.* 2012). This comparison must take into account the uncertainty of the remagnetization direction, which is conditioned by the SCI method. The method gives as solution the direction with minimum parameter *A*, but if variability of bedding strikes between sites is moderate, the area of points with a low *A* value (i.e. area of intersection of SC) is very elongated along the small circles, as can be seen in Figure 8b (*A* contours around the solution). Therefore, in these cases, the uncertainty of the obtained direction is not a confidence circle as a Fisherian population gives, but an elongated, banana-like area. In our case, the uncertainty area is elongated in inclination, but gives good accuracy in declination. In Figure 8a, the mean direction and *A* contours are compared with the expected directions obtained from the GAPWP. The direction obtained by SCI method is close to the expected directions for 100–90 Ma.

The separated declination–age and inclination–age curves (Fig. 9) also confirm this result. Declination gives 100 Ma as the most probably age, with an uncertainty interval between 75 and 110 Ma. Other ages also fit the remagnetization direction (190 and 220 Ma) but they can be discarded because they are older than some remagnetized units. On the other hand, the inclination–age curve does not allow for precise dating because of (1) the indeterminacy of the SCI solution in inclination (elongation of *A* contours) and (2) the low variability in inclination during the Mesozoic. We can conclude that the remagnetization is Late Cretaceous in age, most probably Cenomanian.

This timing is consistent with the other chronological constraints for the remagnetization: (1) it was acquired before the Tertiary compression stage (fold-test results); (2) it is coeval with the Cretaceous Normal Polarity Superchron (systematic normal polarity). On the other hand, our palaeomagnetic result agrees with the early Turonian (*c*. 93 Ma) pole obtained from anoxic, cyclic marine deposits from the Tarfaya coastal basin (SW Morocco; Ruiz-Martínez *et al.* 2011).

Discussion

In the Imilchil transect in the Central High Atlas, the Mesozoic basin is segmented by extensional faults reactivated during tectonic inversion (Fig. 2a). A relationship between the magnetic properties and location within the basin has been demonstrated: the remagnetization (component A, group G1) is observed in outcrops located in the inner part of the basin, limited by the Tizi-n-Isly fault to the north and by the Zabel complex to the south. These extensional faults were active during the Triassic and Early Jurassic rifting stage, and were subsequently reactivated during the Tertiary inversion. These central areas present the maximum thickness of Jurassic rocks (Fig. 2a), reaching 5000 m in the basin depocentre (Teixell *et al.* 2003). On the other hand, outcrops showing characteristics of Group G2 (where the remagnetization component A is absent) are outside this area and correspond to the Mesozoic basin margins, where the Jurassic sediments thickness decreases to 1000 m, north of Tizi-n-Isly and in the Zabel complex faults (Teixell *et al.* 2003).

The relationship between magnetic properties and the position within the basin indicates that the remagnetization process is conditioned by geometry and sediment thickness. Several studies have established a relationship between remagnetization and burial processes (Katz *et al.* 1998; Woods *et al.* 2000, 2002; Evans & Elmore 2006; Aubourg *et al.* 2008, 2012). Some of these studies related sediment burial to mineral transformation and remagnetization (Katz *et al.* 1998; Woods *et al.* 2000). Others invoked pressure solution structures as the driving mechanism of the remagnetization within the burial context (Evans & Elmore 2006). Aubourg *et al*. (2008, 2012) demonstrated that magnetite can form at the expense of pyrite in clays and the possibility that remagnetization can be due to the unique action of temperature during burial. Studies suggest that the remagnetization events can be linked to sediment thickness and depth of burial and consequently can be controlled by the geometry of basins.

The correlation between the occurrence of the remagnetization, the position in the basin and the magnetic properties gives some hints about the remagnetization mechanism. The remagnetized rocks located in the internal parts of the basin presented different magnetic properties and mineralogy (magnetite) from non-remagnetized rocks located in the external units of the basin, suggesting that the magnetite responsible for the remagnetization is authigenic. This indicates that a thermoviscous remagnetization of detrital magnetite can be excluded, whereas a chemical remagnetization involving the growth of new magnetite can be assumed, and is also supported by the observed hysteresis parameters, which are similar to those observed in other chemical remagnetizations (Jackson 1990; Channell & McCabe 1994).

The properties and geometrical relationships of remagnetization in the High Atlas can be related to similar processes in nearby areas. The Iberian Chain, an intracratonic mountain chain located in the Iberian plate, is the counterpart of the Atlas belt on the other side of the African–Iberian plate margin (delimited by the Betic and Rif chains). Both the Iberian Chain and the Atlas resulted from the inversion of Mesozoic basins caused by convergence between Africa and Europe (e.g. Casas & Faccenna 2001) and underwent a basinal evolution characterized by terrigenous deposits during the rifting stages and widespread carbonate platforms during the post-rift periods. Furthermore, particular palaeomagnetic features of the Mesozoic rocks in both ranges allow for a detailed comparison of the data obtained in this study.

Several palaeomagnetic studies have shown that remagnetization events are a phenomenon especially frequent in Mesozoic sediments of Iberia (e.g. Galdeano *et al.* 1989; Moreau *et al.* 1992, 1997; Villalaín *et al.* 1994, 2003; Juárez *et al.* 1998; Dinarès-Turell & García-Senz 2000; Osete *et al.* 2004, 2007; Gong *et al.* 2008*a*; Soto *et al.* 2008, 2011; Casas *et al.* 2009). Most of these overprints have been dated as Cretaceous, similar to the remagnetization of Mesozoic sediments from the High Atlas found in the present study. Examples of these Cretaceous remagnetizations involve not only the Iberian Chain (Maestrazgo basin, Moreau *et al.* 1992; Cameros basin, Villalaín *et al.* 2003; Casas *et al.* 2009; Central Iberian basin, Juárez *et al.* 1998; Osete *et al.* 2007), but also other regions such as the Lusitanian basin (Galdeano *et al.* 1989; Márton *et al.* 2004), and South Pyrenean basins (Organyà basin, Dinarés-Turell & García-Senz 2000; Gong *et al.* 2008*a*; Cabuérniga basin, Soto *et al.* 2008; Polientes basin, Soto *et al.* 2011). These remagnetization events are controversial, and have been linked to two different scenarios: (1) wholesale remagnetization probably linked to subcrustal processes, involving large areas at the plate scale (Juárez *et al.* 1998), or (2) progressive remagnetization linked to the geodynamic evolution of each basin (Gong *et al.* 2009) and associated with sedimentary burial. The first hypothesis is mainly based on similar, Cretaceous, remagnetization ages. On the other hand, comparing the APWP for Iberia with the different declination data from three Mesozoic basins (Gong *et al.* 2009), the second hypothesis implies diachronous events, thus explaining the different directions of remagnetizations obtained in different basins. However, it is difficult to determine the age of remagnetizations in Iberia owing to the low accuracy of the Cretaceous APWP (Neres *et al.* 2013) and because after the Early Cretaceous, declinations in the Iberian plate do not change enough to provide resolution for dating through comparison of palaeomagnetic directions.

The magnetic properties characteristic of samples from group G1 obtained in the Imilchil section of the High Atlas are very similar to those observed in remagnetized limestones from Iberian Mesozoic basins (Juárez *et al.* 1998; Gong *et al.* 2008*a*; Soto *et al.* 2008, 2011; Villalaín *et al.* 2012). They also exhibit a normal polarity component carried probably by magnetite with maximum unblocking temperatures of about 450–500 °C and low to intermediate coercivity (30–100 mT). The thermal demagnetization decay curves show similar shapes, and the ratios of the hysteresis parameters M_{rs}/M_s and H_{cr}/H_c correspond to a mixture of SD and SP magnetite grains, as seen in other studies of carbonate rocks that have undergone chemical remagnetization.

The connection between remagnetization events and burial and its confinement to thick sedimentary basins has been proposed by Gong *et al*. (2009) for the pervasive remagnetizations occurring in Iberia during the Cretaceous. Those researchers supported this model in the variation in the declination of remagnetization directions in four North Iberian basins (Juárez *et al.* 1998; Villalaín *et al.* 2003; Gong *et al.* 2008*a*; Soto *et al.* 2008). This variation is interpreted as generated by diachronous acquisition of remagnetizations in the different basins. Gong *et al*. (2009) dated the overprints by comparing the remagnetization directions with the Cretaceous Iberian rotation chronology proposed by Gong *et al*. (2008*b*). This remagnetization model contradicts the previous hypothesis established by Juárez *et al*. (1998) suggesting that this set of remagnetizations in different areas of Iberia might correspond to a widespread single remagnetization event. Following Gong *et al*. (2009), the four Iberian remagnetizations discussed in their paper occurred at different times during the Iberian rotation and are bracketed within a minimum timespan of about 10–15 Ma, mostly during the Aptian. However, it is important to note that the chronology of the Cretaceous Iberian rotation is based on a low-resolution and low-quality palaeomagnetic database (Neres *et al.* 2012, 2013). In fact, the abundance of remagnetizations in Iberia during the Cretaceous is one of the main reasons for the scarcity of reliable palaeomagnetic data (Osete & Palencia 2006; Osete *et al.* 2011). In addition, evident inconsistencies are observed in the kinematic models obtained from the analysis of sea-floor magnetic anomalies and from palaeomagnetic data for the Early Cretaceous (Neres *et al.* 2012, 2013).

From this diachronous acquisition, Gong *et al*. (2009) concluded that the remagnetization events were confined to single basins, and stated that there is no need to invoke speculative regional plate-scale mechanisms in the sense proposed by Juárez *et al*. (1998). However, although the remagnetizations in the four analysed locations occurred at different times, they are all chronologically related to the rifting phase in their own geological history. The Cretaceous Iberian remagnetization events in northern Iberia are hence temporally related to the extensional tectonics on a regional scale, compatible with the relatively short period of 10–15 Ma within which the remagnetization events are bracketed.

The palaeogeographical proximity between Iberia and the High Atlas basins during Jurassic and Cretaceous times (Vissers & Meijer 2012) and the similarity in magnetic properties and geological contexts suggests a connection between the remagnetization events in Iberia and that observed in the High Atlas. In this sense it is noticeable that the Cenomanian age of the remagnetization in the High

Atlas determined here is very close to the ages found for the set of widespread remagnetizations in Iberia. This result is not compatible with the model proposed by Gong *et al*. (2009) because the widespread remagnetization in the High Atlas clearly postdates the age of maximum extension and accumulation of sediments in this area. The maximum rifting phase in the Iberian basins corresponds to the Early Cretaceous with strongly subsiding continental and marine basins followed by fluvial and deltaic sedimentation during the Albian–Cenomanian, coeval with remagnetizations. However, in the High Atlas the maximum extensional tectonics occurred during Early to Middle Jurassic times, whereas the remagnetization is dated at the beginning of the Late Cretaceous, coinciding with the same process in the Iberian basins. The geological context is very similar in both areas, with intraplate extensional structures and remagnetized basins; the ages of the remagnetizations are similar and the magnetic properties have analogous characteristics. This evidence suggests that a common regional agent must control the remagnetizations observed in Iberia and North Africa, thus supporting the hypothesis of a regional event in the sense suggested by Juárez *et al*. (1998).

However, in this paper we also show evidence supporting the confinement of remagnetization to a basin scale and the connection between remagnetization and evolution of each basin, with boundary conditions of burial necessary for the occurrence of the remagnetization event. This suggests that a more complex scenario with two geological requirements is needed to generate these widespread regional remagnetizations in the Cretaceous, as follows.

(1) Basin-scale conditions. The widespread chemical remagnetization in the High Atlas is controlled by the geometry of the basin and it can be observed only in sediments that underwent a minimum depth of burial during the basinal stage. This indicates that the remagnetization process occurs at the scale of each sedimentary basin as suggested by Gong *et al*. (2009).

(2) Regional-scale thermal event. A regional agent must activate or favour the generation of remagnetizations in Mesozoic sedimentary basins that satisfy the basin-scale conditions. This regional event can explain the synchronous remagnetizations reported in Iberia and in the High Atlas, despite the differences in chronology of the evolution of each basin.

Which is the regional catalyst of remagnetization episodes? Although no particularly significant tectonic events occurred in the study area (nor in the Iberian Chain) during the proposed remagnetization interval, the magmatic and thermal evolution of the High Atlas can give some insights into the mechanisms involved in this process. Barbero *et al*. (2007), on the basis of fission-track analysis, proposed a thermal history with a slow cooling period (or even heating, in samples from the northern margin of the High Atlas) between 120 and 80 Ma. This slow cooling can be coupled with the thermal events witnessed by magmatic intrusions and lava flows that are persistent during the Mesozoic period (Michard *et al.* 2008) and are consistent with a large-scale thermal anomaly. These thermal and magmatic events, probably linked to mantle sources, could have been able to provoke a chemically driven remagnetization mechanism. The elevation of geothermal gradients at a regional scale may provide the diagenetic temperatures required for generation of secondary magnetite in sediments located in basins with a critical amount of sediments, which thus reached greater depths. This thermal event could develop and end during the Normal Polarity Superchron, thus explaining the systematic normal polarity in the remagnetizations observed in the Mesozoic basins of Iberia and North Africa. The age of remagnetizations reflects not the complete event but rather its end.

Models explaining the opening of the Central Atlantic during the Triassic are consistent with high thermal gradients, rifting and crustal thinning related to the Central Atlantic Magmatic Province magmatism, whose relation with a large-scale mantle plume is still under debate (see e.g. Hill 1991; McHone *et al.* 2005; Nomade *et al.* 2007; Ruiz-Martínez *et al.* 2012). A different and more localized mechanism, although at a regional scale as the area involved is at least 1500 km wide, can be invoked for the development of isochronous widespread remagnetizations under a wholesale rifting process during the Cretaceous in the western Tethys. Rifting in the Tethyan margin of the Iberian plate and the Alpine Tethys (see, e.g. Stampfli & Borel 2002, 2003; Antolín-Tomás *et al.* 2007, and references therein) could be responsible for a thermal anomaly that could outlive rifting and last during the plate reorganization at the end of the Early Cretaceous in the Iberian–African realm (Dewey *et al.* 1989; Sengör 2009), roughly coeval with the end of the remagnetization processes. However, the connection of Alpine Tethyan rifting with extensional basins in North Africa is not straightforward (Biju-Duval *et al.* 1977; Hay *et al.* 1999), thus favouring an alternative model in which subcrustal dynamics is responsible for the thermal anomaly, not incompatible with extension and rifting (see, e.g. Cloetingh *et al.* 2011), and with the relatively long timespan of remagnetization processes in Iberia and North Africa.

Conclusions

This study provides the first palaeomagnetic data for Mesozoic sediments of the Central High Atlas. The synrift sediments, consisting of Jurassic limestones and marly limestones, underwent a pervasive remagnetization with systematic normal polarity.

Fold-tests indicate that this overprint is syn-folding in some structures but clearly predates the Tertiary compression stage. By using the small circle intersection method, the palaeomagnetic direction at the acquisition time has been calculated ($D = 336.4°$, $I = 29.2°$, $k = 36.3$, $\alpha_{95} = 4.1°$). Comparing this direction with those expected from GAPWP running means in Africa coordinates (Torsvik *et al.* 2012), we have obtained the most probable age of the remagnetization in the Imilchil transect as Cenomanian. This age is consistent with the fold-test results and coeval with the Cretaceous Normal Polarity Superchron.

A relationship between the magnetic properties and location within the basin has been obtained, suggesting that the acquisition of the remagnetization is controlled by geometry. The remagnetization is observed along a 70 km wide belt, where the thickness of the Mesozoic series has higher values (about 5 km). This remagnetized area is limited by major tectonic structures inherited from the basinal stage. Outside this area the Mesozoic series show different magnetic properties and do not register the remagnetization. This behaviour suggests that the overprint is a chemical remagnetization linked to the generation of secondary magnetite related to sediment burial processes.

The remagnetized rocks of the High Atlas exhibit the same magnetic behaviour as those observed in remagnetized limestones from Iberian basins: the carrier of the NRM is magnetite with maximum unblocking temperatures of 450–475 °C, low to intermediate coercivity, and the magnetic mineralogy is dominated by a mixture of SD + SP magnetite grains. In addition, the timing of the remagnetization in the High Atlas is the same as that of the systematic remagnetizations observed in the Iberian Mesozoic basins, despite the different age of the main rifting process.

Considering both the basinal confinement of remagnetization and the connection with other remagnetization events in the western Tethys, we propose a scenario explaining widespread remagnetizations in the region, involving (1) basin-scale conditions mainly related to a minimum thickness of sediments and (2) a regional-scale thermal event acting as a catalyst of remagnetization events in those sedimentary basins that satisfy the basin-scale conditions.

This proposal brings into line the hypotheses proposed to explain the set of remagnetizations in the region: a regional thermal event (Juárez *et al.* 1998) versus progressive remagnetization linked to the geodynamic evolution of each basin (Gong *et al.* 2009).

We thank A. Morris and M. Mattei for their valuable comments, which improved the paper. Funding for this work came from projects CGL 2009-10840, CGL2009-08969 and CGL2012-38481 of the Dirección General de Investigación Científica y Técnica, Ministerio de Economía y Competitividad of the Spanish government. S.T.-L. acknowledges the financial support given by the grant of FPI by the Ministerio de Economía y Competitividad of the Spanish government. We thank C. R. Nieto and A. Mahmoudi for their help in the fieldwork.

References

Antolín-Tomás, B., Liesa, C.L., Casas, A.M. & Gil-Peña, I. 2007. Geometry of fracturing linked to extension and basin formation in the Maestrazgo basin (Eastern Iberian Chain, Spain). *Revista de la Sociedad Geológica de España*, **20**, 351–365.

Appel, E., Crouzet, C. & Schill, E. 2012. Pyrrhotite remagnetizations in the Himalaya: a review. *In*: Elmore, R.D., Muxworthy, A.R., Aldana, M.M. & Mena, M. (eds) *Remagnetization and Chemical Alteration of Sedimentary Rocks*. Geological Society, London, Special Publications, **371**, 163–180.

Aubourg, C., Pozzi, J.-P., Janots, D. & Sarahoui, L. 2008. Imprinting chemical remanent magnetization in claystones at 95 °C. *Earth and Planetary Science Letters*, **272**, 172–180.

Aubourg, C., Pozzi, J.-P. & Kars, M. 2012. Burial, claystones remagnetizations and some consequences for magnetistratigraphy. *In*: Elmore, R.D., Muxworthy, A.R., Aldana, M.M. & Mena, M. (eds) *Remagnetization and Chemical Alteration of Sedimentary Rocks*. Geological Society, London, Special Publications, **371**, 181–188.

Ayarza, P., Alvarez-Lobato, F., Teixell, A., Arboleya, M.L., Tesón, E., Julivert, M. & Charroud, M. 2005. Crustal structure under the central High Atlas Mountains (Morocco) from geological and gravity data. *Tectonophysics*, **400**, 67–84.

Barbero, L., Teixell, A., Arboleya, M.-L., Del Rio, P., Reiners, P.W. & Bougadir, B. 2007. Jurassic-to-present thermal history of the central High Atlas (Morocco) assessed by low-temperature thermochronology. *Terra Nova*, **19**, 58–64, http://dx.doi.org/10.1111/j.1365-3121.2006.00715.x.

Beauchamp, W., Allmendinger, R.W., Barazangi, A., Demnati, A., El Alji, M. & Dahmani, M. 1999. Inversion tectonics and the evolution of the High Atlas Mountains, Morocco, based on a geological–geophysical transect. *Tectonics*, **18**, 163–184.

Benammi, M., Toto, E. & Chakiri, S. 2001. Les chevauchements frontaux du Haut Atlas central marocain: Styles structuraux et taux de raccourcissement différentiel entre les versants nord et sud. *Comptes Rendus de l'Académie des Sciences*, **333**, 241–247.

Biju-Duval, B., Dercourt, J. & LePichon, X. 1977. From the Tethys Ocean to the Mediterranean seas: a plate tectonic model of the evolution of the Western Alpine system. *In*: Biju-Duval, B. & Montadert, L. (eds) *International Symposium on the Structural History of the Mediterranean Basins, Split (Yugoslavia)*. Technip, Paris, 143–164.

Bracène, R. & Frizon de Lamotte, D. 2002. The origin of intraplate deformation in the Atlas system of western and central Algeria: From Jurassic rifting to Cenozoic–Quaternary inversion. *Tectonophysics*, **357**, 207–226.

Cairanne, G., Aubourg, C. & Pozzi, J.P. 2002. Syn-folding remagnetization and the significance of the small circle. Examples from the Vocontian trough (SE France). *Physics and Chemistry of the Earth*, **27**, 1151–1159.

Casas, A.M. & Faccenna, C. 2001. Tertiary compressional deformation of the Iberian plate. *Terra Nova*, **13**, 281–288.

Casas, A.M., Villalaín, J.J., Soto, R., Gil-Imaz, A., Del Río, P. & Fernández, G. 2009. Multidisciplinary approach to an extensional syncline model for the Mesozoic Cameros Basin (N Spain). *Tectonophysics*, **470**, 3–20.

Channell, J.E.T. & McCabe, C. 1994. Comparison of magnetic hysteresis parameters of unremagnetized and remagnetized limestones. *Journal of Geophysical Research*, **99**, 4613–4623.

Choubert, G. & Faure-Muret, A. 1962. Evolution du domaine atlasique marocain depuis les temps paléozoïques. *In*: *Evolution du domaine atlasique marocain depuis les temps paléozoïques, livre à la mémoire du Prof. P. Fallot*. Mémoire hors-série, Service de la Société Géologique de France, **1**, 447–514.

Cloetingh, S., Gallart, J., de Vicente, G. & Matenco, L. 2011. TOPO-EUROPE: From Iberia to the Carpathians and analogues. *Tectonophysics*, **502**, 1–27.

Day, R., Fuller, M.D. & Schmidt, V.A. 1977. Hysteresis properties of titanomagnetites: Grain size and composition dependence. *Physics of the Earth and Planetary Interiors*, **13**, 260–267.

Dewey, J.F., Helman, M.L., Turco, E., Hutton, D.H.W. & Knott, S.D. 1989. Kinematics of the western Mediterranean. *In*: Coward, M.P., Dietrich, D. & Park, R.G. (eds) *Alpine Tectonics*. Geological Society, London, Special Publications, **45**, 265–283.

Dinarès-Turell, J. & García-Senz, J. 2000. Remagnetization of Lower Cretaceous limestones from the southern Pyrenees and relation to the Iberian plate geo-dynamic evolution. *Journal of Geophysical Research*, **105B**, 19405–19418.

Donald, P.C., Van der Voo, R. & Van der Pluijm, B. 2006. Syn-folding remagnetization of Cambro-Ordovician carbonates from the Pennsylvania Salient post-dates oroclinal rotation. *Tectonophysics*, **422**, 41–54.

Dunlop, D.J. 2002. Theory and application of the Day plot (M_{rs}/M_s versus H_{cr}/H_c): 2. Application to data for rocks, sediments, and soils. *Journal of Geophysical Research*, **107**, http://dx.doi.org/10.1029/2001JB000487.

El Harfi, A., Lang, J., Salomon, J. & Chellai, 2001. Cenozoic sedimentary dynamics of the Ouarzazate foreland basin (central High Atlas Mountains, Morocco). *International Journal of Earth Science*, **90**, 393e411.

El Harfi, A., Guiraud, M. & Lang, J. 2006. Deep-rooted 'thick skinned' model for the High Atlas Mountains (Morocco). Implications for the structural inheritance of the southern Tethys passive margin. *Journal of Structural Geology*, **28**, 1958–1976, http://dx.doi.org/10.1016/j.jsg.2006.08.011.

Ellero, A., Ottria, G., Malusà, M.G. & Ouanaimi, H. 2012. Structural geological analysis of the High Atlas (Morocco): Evidences of a transpressional fold–thrust belt. *In*: Sharkov, E. (ed.) *Tectonics—Recent Advances*. InTech, Rijeka, 229–258, http://dx.doi.org/10.5772/50071.

Enkin, R.J., Wheadon, P.M., Baker, J. & Osadetz, K.G. 1997. Paleomagnetic constraints on the tectonic history of the Foreland Belt, southern Canadian Cordillera: preliminary results. *Canadian Journal of Earth Sciences*, **34**, 260–270.

Enkin, R.J., Osadetz, K.G., Baker, J. & Kisilevsky, D. 2000. Orogenic remagnetizations in the front ranges and inner foothills of the Southern Canadian Cordillera: Chemical harbinger and thermal handmaiden of Cordilleran deformation. *Geological Society of America Bulletin*, **112**, 929–942.

Evans, M.A., Elmore, R.D. & Lewchuk, M.T. 2000. Examining the relationship between remagnetization and orogenic fluids: Central Appalachians. *Journal of Geochemical Exploration*, **69–70**, 139–142.

Evans, M.A. & Elmore, R.D. 2006. Fluid control of localized mineral domains in limestone pressure solution structures. *Journal of Structural Geology*, **28**, 284–301.

Fisher, R.A. 1953. Dispersion on a sphere. *Proceedings of the Royal Society of London, Series A*, **217**, 295–305.

Frizon de Lamotte, D., Saint Bézar, B., Bracène, R. & Mercier, E. 2000. The two main steps of the Atlas building and geodynamics of the western Mediterranean. *Tectonics*, **19**, 740–761.

Frizon de Lamotte, D., Leturmy, P., *et al.* 2008. Mesozoic and Cenozoic vertical movements in the Atlas system (Algeria, Morocco, Tunisia): An overview. *Tectonophysics*, **475**, 9–28.

Galdeano, A., Moreau, M.G., Pozzi, J.P., Berthou, P.Y. & Malod, J.A. 1989. New paleomagnetic results from Cretaceous sediments near Lisboa (Portugal) and implications for the rotation of Iberia. *Earth and Planetary Science Letters*, **92**, 95–106.

Gong, Z., Dekkers, M.J., Dinarès-Turell, J. & Mullender, T.A.T. 2008*a*. Remagnetization mechanism of lower Cretaceous rocks from the Organyà basin (Pyrenees, Spain). *Studia Geophysica et Geodaetica*, **52**, 187–210.

Gong, Z., Langereis, C.G. & Mullender, T.A.T. 2008*b*. The rotation of Iberia during the Aptian and the opening of the Bay of Biscay. *Earth and Planetary Science Letters*, **273**, 80–93.

Gong, Z., Van Hinsbergen, D.J.J. & Dekkers, M.J. 2009. Diachronous pervasive remagnetization in northern Iberian basins during Cretaceous rotation and extension. *Earth and Planetary Science Letters*, **284**, 292–301.

Hay, W.W., De Conto, R., *et al.* 1999. Alternative global Cretaceous paleogeography. *In*: Barrera, E. & Johnson, C.C. (eds) *Evolution of the Cretaceous Ocean–Climate System*. Geological Society of America, Special Papers, **332**, 1–47.

Henry, B., Rouvier, H. & Le Goff, M. 2004. Using syntectonic remagnetizations for fold geometry and vertical axis rotation: The example of the Cévennes border (France). *Geophysical Journal International*, **157**, 1061–1070.

Hill, I.R. 1991. Starting plumes and continental break-up. *Earth and Planetary Science Letters*, **104**, 398–416.

Ibouh, I., Bouabdelli, M. & Zargouni, F. 1994. Indices de tectonique synsédimentaire dans les dépôts aalénobajociens de la région d'Imilchil (Haut Atlas central, Maroc). *In*: Cresta, S. & Pavia, G. (eds) *Proceedings of the 3rd International Meeting on Aalenian and Bajocian Stratigraphy, Marrakesh, May 1994*. Istituto poligrafico e Zecca dello Stato, Rome, 305–309.

Jackson, M. 1990. Diagenetic sources of stable remanence in remagnetized Paleozoic cratonic carbonates: a rock magnetic study. *Journal of Geophysical Research.*, **95**, 2753–2761.

Juárez, M.T., Lowrie, W., Osete, M.L. & Meléndez, G. 1998. Evidence of widespread Cretaceous remagnetisation in the Iberian Range and its relation with the rotation of Iberia. *Earth and Planetary Science Letters*, **160**, 729–743.

Katz, B., Elmore, R.D., Cogoini, M. & Ferry, S. 1998. Widespread chemical remagnetization: orogenic fluids or burial diagenesis of clays? *Geology*, **26**, 603–606.

Kent, D.V. 1985. Thermoviscous remagnetization in some Appalachian limestones. *Geophysical Research Letters*, **12**, 805–808.

Laville, E., Lesage, J.L. & Séguret, M. 1977. Géométrie, cinématique (dynamique) de la tectonique atlasique sur le versant sud du Haut Atlas marocain. Aperçu sur les tectoniques hercyniennes et tardi-hercyniennes. *Bulletin de la Société Géologique de France*, **7**, 499–523.

Laville, E. & Harmand, C. 1982. Évolution magmatique et tectonique du bassin intracontinental mésozoïque du Haut Atlas (Maroc): Un modèle de mise en place synsédimentaire de massifs anorogéniques liés à des décrochements. *Bulletin de la Société Géologique de France*, **24**, 213–227.

Laville, E. & Piqué, A. 1992. Jurassic penetrative deformation and Cenozoic uplift in the central High Atlas (Morocco): A tectonic model. Structural and orogenic inversions. *Geologische Rundschau*, **81**, 157–170.

Laville, E. 2002. Role of Atlas Mountains (northwest Africa) within the African–Eurasian plate-boundary zone: Comment. *Geology*, **30**, 95.

Laville, E., Piqué, A., Amrhar, M. & Charroud, M. 2004. A restatement of the Mesozoic Atlasic Rifting (Morocco). *Journal of African Earth Sciences*, **38**, 145–153.

Lewchuk, M.T., Evans, M.A. & Elmore, R.D. 2002. Remagnetization signature of Paleozoic sediments from the Patterson Creek anticline in West Virginia. *Physics and Chemistry of the Earth*, **27**, 1141–1150.

Lowrie, W. 1990. Identification of ferromagnetic minerals in a rock by coercivity and unblocking temperature properties. *Geophysical Research Letters*, **17**, 159–162.

Márton, E., Abranches, M.C. & Pais, J. 2004. Iberia in the Cretaceous: new paleomagnetic results from Portugal. *Journal of Geodynamics*, **38**, 209–221.

Mattauer, M., Proust, F. & Tapponier, P. 1972. Major strike-slip fault of late Hercynian age in Morocco. *Nature*, **237**, 160–162.

Mattauer, M., Tapponier, P. & Proust, F. 1977. Sur les mécanismes de formation des chaînes intracontinentales. L'exemple des chaînes atlasiques du Maroc. *Bulletin de la Société Géologique de France*, **19**, 521–526.

McCabe, C. & Elmore, R.D. 1989. The occurrence and origin of late Paleozoic remagnetization in the sedimentary rocks of North America. *Reviews of Geophysics*, **27**, 471–494.

McFadden, P.L. & Jones, D.L. 1981. The fold test in palaeomagnetism. *Geophysical Journal of the Royal Astronomical Society*, **67**, 53–58.

McHone, J.G., Anderson, D.L., Beutel, E.K. & Fialko, Y.A. 2005. Giant dikes, rifts, flood basalts, and plate tectonics: A contention of mantle models. *In*: Geological Society of America, Special Papers, **388**, 401–420.

Michard, A., Saddiqi, O., Chalouan, A. & Frizon de Lamotte, D. (eds) 2008. *Continental Evolution: The Geology of Morocco. Structure, Stratigraphy, and Tectonics of the African–Atlantic–Mediterranean Triple Junction*. Lecture Notes in Earth Sciences, **116**.

Missenard, Y. 2006. *Le relief des atlas marocains: contribution des processus asthénosphériques et du raccourcissement crustal, Aspects chronologiques*. Thèse de doctorat, Université de Cergy Pontoise.

Moreau, M.G., Canérot, J. & Malod, J.A. 1992. Paleomagnetic study of Mesozoic sediments from the Iberian Chain (Spain): Suggestions for Barremian remagnetization and implications for the rotation of Iberia. *Bulletin de la Société Géologique de France*, **163**, 393–402.

Moreau, M.G., Berthou, P.Y. & Malod, J.A. 1997. New paleomagnetic Mesozoic data from the Algarve (Portugal): Fast rotation of Iberia between the Hauterivian and the Aptian. *Earth and Planetary Science Letters*, **146**, 689–701.

Neres, M., Font, E., Miranda, J.M., Camps, P., Terrinha, P. & Mirão, J. 2012. Reconciling Cretaceous paleomagnetic and marine magnetic data for Iberia: New Iberian paleomagnetic poles. *Journal of Geophysical Research*, **117**, http://dx.doi.org/10.1029/2011JB009067.

Neres, M., Miranda, J.M. & Font, E. 2013. Testing Iberian kinematics at Jurassic–Cretaceous times. *Tectonics*, http://dx.doi.org/10.1002/tect.20074.

Nomade, S., Knight, K.B., et al. 2007. The chronology of CAMP: relevance for the central Atlantic rifting processes and the Triassic–Jurassic biotic crisis. *Palaeogeography, Palaeoclimatology, Palaeoecology*, **244**, 326–344.

Oliva-Urcia, B., Pueyo, E.L. & Larrasoaña, J.C. 2007. Magnetic reorientation induced by pressure solution: a potential mechanism for orogenic-scale remagnetizations. *Earth and Planetary Science Letters*, **265**, 525–534.

Osete, M.L., Villalaín, J.J., Palencia, A., Sandoval, J. & García Dueñas, V. 2004. New paleomagnetic data from the Betic Cordillera: Constraints on the timing and the geographical distribution of tectonics rotations in southern Spain. *Pure and Applied Geophysics*, **161**, 701–722.

Osete, M.L. & Palencia, A. 2006. Polos Paleomagnéticos de Iberia de los últimos 300 millones de años. *Física de la Tierra*, **18**, 157–181.

Osete, M.L., Gialanella, P.R., Gómez, J.J., Villalaín, J.J., Goy, A. & Heller, F. 2007. Magnetostratigraphy of Early–Middle Toarcian expanded sections from the Iberian Range (Central Spain). *Earth and Planetary Science Letters*, **259**, 319–332.

Osete, M.L., Gómez, J.J., Carrasco, F.J., Villalaín, J.J., Palencia, A., Ruíz-Martínez, V.C. & Heller, F. 2011. The evolution of Iberia during the Jurassic from paleomagnetic data. *Tectonophysics*, **502**, 105–120.

Piqué, A., Charroud, M., Laville, E. & Amrhar, M. 2000. The Tethys Southern Margin in Morocco: Mesozoic and Cenozoic Evolution of the Atlas Domain. *Mémoires du Muséum National d'Histoire Naturelle*, **182**, 93–106.

Ruiz-Martínez, V.C., Palencia-Ortas, A., Villalain, J.J., McIntosh, G. & Martin-Hernández, F. 2011. Palaeomagnetic and AMS study of the Tarfaya coastal basin, Morocco: An early Turonian palaeopole for the African plate. *In*: van Hinsbergen, D.J.J., Buiter, S.J.H., Torsvik, T.H., Gaina, C. & Webb, S.J. (eds) *The Formation and Evolution of Africa: A Synopsis of 3.8 Ga of Earth History*. Geological Society, London, Special Publications, **357**, 211–227.

Ruiz-Martínez, V.C., Torsvik, T.H., Van Hinsbergen, D.J.J. & Gaina, C. 2012. Earth at 200 Ma: Global palaeogeography refined from CAMP palaeomagnetic data. *Earth and Planetary Science Letters*, **331–332**, 67–79, http://dx.doi.org/10.1016/j.epsl.2012.03.008.

Roberts, A.P., Cui, Y. & Verosub, K.L. 1995. Waspwaisted hysteresis loops: mineral magnetic characteristics and discrimination of components in mixed magnetic systems. *Journal of Geophysical Research*, **100**, 17909–17924.

Scotese, C.R., Van der Voo, R. & McCabe, C. 1982. Paleomagnetism of the Upper Silurian and Lower Devonian carbonates of New York State: Evidence for secondary magnetizations residing in magnetite. *Physics of the Earth and Planetary Interiors*, **30**, 385–395.

Sengör, A.M.C. 2009. Tectonic evolution of the Mediterranean: A dame with four husbands. *Trabajos de Geología, Universidad de Oviedo*, **29**, 45–50.

Shipunov, S.V. 1997. Synfolding magnetization: Detection, testing and geological applications. *Geophysical Journal International*, **130**, 405–410.

Sibuet, J.-C., Rouzo, S. & Srivastava, S. 2012. Plate tectonic reconstructions and paleogeographic maps of the central and North Atlantic oceans. *Canadian Journal of Earth Sciences*, **49**, 1395–1415.

Soto, R., Casas-Sainz, A.M., et al. 2008. Characterizing the Mesozoic extension direction in the Northern Iberian Plate margin by anisotropy of magnetic susceptibility (AMS). *Journal of the Geological Society, London*, **165**, 1007e1018.

Soto, R., Casas-Sainz, A.M. & Villalaín, J.J. 2011. Widespread Cretaceous inversion event in northern Spain; evidence from subsurface and paleomagnetic data. *Journal of the Geological Society, London*, **168**, 899e912.

Stamatakos, J., Hirt, A.M. & Lowrie, W. 1996. The age and timing of folding in the central Appalachians from paleomagnetic results. *Geological Society of America Bulletin*, **108**, 815–829.

Stampfli, G.M. & Borel, G.D. 2002. A plate tectonic model for the Paleozoic and Mesozoic constrained by dynamic plate boundaries and restored synthetic oceanic isochrons. *Earth and Planetary Science Letters*, **196**, 17–33.

Stampfli, G.M. & Borel, G. 2003. A revised plate tectonic model for the western Tethys from Paleozoic to Cretaceous. *In: Book of Abstracts of AAPG International Conference, Barcelona, Spain, September 21-24, 2003*. EGS/AGU/EUG joint assembly, Nice, EAE03-A-10205.

Teixell, A., Arboleya, M.L., Julivert, M. & Charroud, M. 2003. Tectonic shortening and topography in the central High Atlas (Morocco). *Tectonics*, **22**, 1051, http://dx.doi.org/10.1029/ 2002TC001460.

Teixell, A., Ayarza, P., Zeyen, H., Fernandez, M. & Arboleya, M.L. 2005. Effects of mantle upwelling in a compressional setting: The Atlas Mountains of Morocco. *Terra Nova*, **17**, 456–461.

Tohver, E., Weil, A.B., Solum, J.G. & Hall, C.M. 2008. Direct dating of carbonate remagnetization by ^{40}Ar/^{39}Ar analysis of the smectite–illite transformation. *Earth and Planetary Science Letters*, **274**, 524–530.

Torsvik, T.H., Van der Voo, R., et al. 2012. Phanerozoic polar wander, palaeogeography and dynamics. *Earth-Science Reviews*, **114**, 325–368.

Tucker, S. & Kent, D.V. 1988. Multiple remagnetizations of the lower Paleozoic limestones from the Taconics of Vermont. *Geophysical Research Letters*, **15**, 1251–1254.

Van der Voo, R. & Torsvik, T.H. 2012. The history of remagnetization of sedimentary rocks: deceptions, developments and discoveries. *In*: Elmore, R.D., Muxworthy, A.R., Aldana, M.M. & Mena, M. (eds) *Remagnetization and Chemical Alteration of Sedimentary Rocks*. Geological Society, London, Special Publications, **371**, 23–53.

Valet, J.P., Soler, V. & Courtillot, V. 1998. Remagnetization in lava flows recording pretransitional directions. *Journal of Geophysical Research*, **103**, 9755–9775.

Villalaín, J.J., Osete, M.L., Vegas, R., García-Dueñas, V. & Heller, F. 1994. Widespread Neogene remagnetization in Jurassic limestones of the south Iberian paleomargin (Western Betics, Gibraltar Arc). *Physics of the Earth and Planetary Interiors*, **85**, 15–33.

Villalaín, J.J., Fernández-Gonzalez, G., Casas, A.M. & Gil-Imaz, A. 2003. Evidence of a Cretaceous remagnetization in the Cameros Basin (North Spain): implications for basin geometry. *Tectonophysics*, **377**, 101–117.

Villalaín, J.J., Casas-Sainz, A., Soto, R. & Torres-López, S. 2012. The widespread Cretaceous remagnetizations in Mesozoic intraplate basins from Iberia and North Africa. Contribution to tectonic studies. *Contributions to Geophysics and Geodesy*, **42**, 121–122.

Vissers, R.L.M. & Meijer, P.Th. 2012. Mesozoic rotation of Iberia: subduction in the Pyrenees? *Earth-Science Reviews*, **110**, 93–110.

Waldhör, M. & Appel, E. 2006. Intersections of remanence small circles: new tools to improve data processing and interpretation in palaeomagnetism. *Geophysical Journal International*, **166**, 33–45.

Woods, S.D., Elmore, R.D. & Engel, M.H. 2000. The occurrence of pervasive chemical remanent magnetizations in sedimentary basins: Implications for dating burial diagenetic events. *Journal of Geochemical Exploration*, **69–70**, 381–385.

Woods, S.D., Elmore, R.D. & Engel, M.H. 2002. Paleomagnetic dating of the smectite-to-illite conversion: Testing the hypothesis in Jurassic sedimentary rocks, Skye, Scotland. *Journal of Geophysical Research*, **107**, http://dx.doi.org/10.1029/2000JB000053.

Zeyen, H., Ayarza, P., Fernández, M. & Rimi, A. 2005. Lithospheric structure under the western African–European plate boundary: A transect across the Atlas Mountains and the Gulf of Cadiz. *Tectonics*, **24**, TC2001, http://dx.doi.org/10.1029/ 2004TC001639.

Received 13 September 2013; revised typescript accepted 20 March 2014.
Scientific editing by Conall Mac Niocaill.